Received: 11 December 2020 | Accepted: 4 May 2021

DOI: 10.1111/jfb.14777

REGULAR PAPER

JOURNAL OF FISH BIOLOGY fsbi

Two new species of *Hypostomus* suckermouth-armoured catfishes (Teleostei: Loricariidae) from central Brazil

Yan F. F. Soares[1,2] | Pedro De Podestà Uchôa de Aquino[2] | Justin C. Bagley[3,4] | Francisco Langeani[5] | Guarino R. Colli[2]

[1]Programa de Pós-Graduação em Ecologia, Instituto de Ciências Biológicas, Universidade de Brasília, Brasília, Brazil

[2]Departamento de Zoologia, Instituto de Ciências Biológicas, Universidade de Brasília, Brasília, Brazil

[3]Department of Biology, Jacksonville State University, Jacksonville, Alabama

[4]Department of Biology, Virginia Commonwealth University, Richmond, Virginia

[5]Departamento de Zoologia e Botânica, Instituto de Biociências, Letras e Ciências Exatas, UNESP – Universidade Estadual Paulista, São José do Rio Preto, Brazil

Correspondence
Yan F. F. Soares, Departamento de Zoologia, Instituto de Ciências Biológicas, Universidade de Brasília, 70910-900 Brasília, DF, Brazil.
Email: yfellipe@gmail.com

Funding information
Conselho Nacional de Desenvolvimento Científico e Tecnológico (CNPq), Grant/Award Number: 305756/2018-4; Coordenação de Apoio à Formação de Pessoal de Nível Superior (CAPES); Fundação de Apoio à Pesquisa do Distrito Federal (FAPDF), Grant/Award Number: 00193.00000926/2018-86; USAID PEER programme, Grant/Award Number: AID-OAA-A-11-00012

Abstract

This study describes two new endemic *Hypostomus* species from central Brazil, which were previously identified as genetically distinct lineages in a recent genomic study that recommended their testing and potential description based on morphological data. A machine learning classification procedure (*random forest*) was used to investigate morphological variation and identify putatively diagnostic characters for these candidate species and revealed that each is morphologically distinct. The new species *Hypostomus cafuringa* is characterized by small size, dark spots under a light background, deeper caudal peduncle and shorter first ray of the pectoral fin and base of the dorsal fin when compared to congeneric species from the region. *H. cafuringa* is known from the headwaters of the Maranhão River, upper Tocantins River basin, Distrito Federal, Brazil. The second new species, *Hypostomus crulsi*, is characterized by dark spots under a light background, absence of plates along the abdomen region, shorter first ray of the pelvic fin, shorter first ray of the pectoral fin and smaller body size. *H. crulsi* is known from the headwaters of the São Bartolomeu River, upper Paraná River basin, Distrito Federal, Brazil. The rapid conversion of natural habitats for agricultural development and the isolation of protected areas represent a serious threat to the continued existence of these two newly described endemic species, which warrant conservation assessment.

KEYWORDS
Hypostominae, Neotropical fishes, Siluriformes, taxonomy

1 | INTRODUCTION

Freshwater fishes in the order Siluriformes, popularly known as "catfishes", constitute among the most diverse groups of teleost fishes worldwide and include *c.* 4100 described species or *c.* 12% of total teleost diversity (Ferraris, 2007; Fricke *et al.*, 2019). Catfishes are cosmopolitan in geographical distribution, predominantly inhabit fresh waters and are characterized by a cylindrical body flattened ventrally for benthic feeding; the absence of scales; presence of barbels on the snout, sides of the mouth and chin; and modifications to the Weberian apparatus for sound production (Bruton, 1996). With *c.* 140 recognized species, the genus *Hypostomus* Lacépède 1803 (Loricariidae: Hypostominae) is one of the most species-rich genera within Siluriformes (Froese & Pauly, 2019). *Hypostomus* species distributions span a broad geographical area from Central America to the southern cone of South America east of the Andes, and the greatest wealth of species in the genus is harboured in the Amazon/Orinoco ecoregion (Cardoso *et al.*, 2021; Jardim de Queiroz *et al.*, 2020; Silva *et al.*, 2016; Zawadzki *et al.*, 2010).

Despite the high species richness of the genus, phylogenetic interrelationships among *Hypostomus* species remain relatively unclear, as studies using morphological and molecular data have had difficulty resolving species into well-supported monophyletic groups (Armbruster, 2004; Montoya-Burgos, 2003; Roxo *et al.*, 2019), and

most studies have used incomplete taxon sampling. Several molecular phylogenies have obtained *Hypostomus* as a monophyletic group (Roxo *et al*., 2019; Silva *et al*., 2016). Most recently, the hypothesis that *Hypostomus* represents a monophyletic group was corroborated by Jardim de Queiroz *et al*. (2020) based on a combined analysis of morphology and multilocus DNA sequence data in a Bayesian multi-species coalescent framework. In their study, which analysed 108 *Hypostomus* species and 35 out-groups, Jardim de Queiroz *et al*. (2020) identified four main clades (which they termed "super-groups") namely the *Hypostomus cochliodon*, *Hypostomus hemiurus*, *Hypostomus auroguttatus* and *Hypostomus plecostomus* super-groups, each defined by a series of diagnostic morphological characters.

Recently, five new *Hypostomus* species were described from the region of central Brazil known as the Central Brazilian Highlands (Alkmim, 2015), namely *Hypostomus denticulatus* Zawadzki *et al*., 2008b, *Hypostomus heraldoi* Zawadzki *et al*., 2008b and *Hypostomus yaku* Martins *et al*., 2014, found in the upper Paraná River basin, as well as *Hypostomus faveolus* Zawadzki *et al*., 2008a, and *Hypostomus delimai* Zawadzki *et al*., 2013, found in the Tocantins–Araguaia River basin (Martins *et al*., 2014; Zawadzki *et al*., 2008a; Zawadzki *et al*., 2008b; Zawadzki *et al*., 2013). This region of central Brazil is drained by the headwater streams of three major watersheds: the Tocantins, Paraná and São Francisco rivers (Barros, 1993). Headwater streams of these basins are mainly inhabited by small-sized fishes and exhibit high species endemism (Aquino & Colli, 2017; Castro, 1999). Seven species of restricted distribution were identified as occurring only in the Distrito Federal region of central Brazil in recent surveys (Aquino & Couto, 2010; Nogueira *et al*., 2010).

Applications of molecular techniques in systematics and alpha-taxonomy studies have increased and contributed greatly to the identification and description of new species over the past 30 years, especially through revealing a large number of cryptic species, *i.e*., two or more distinct species misclassified as one species due to superficial morphological resemblance, as well as information on the timing of species divergences (Bickford *et al*., 2007; Cardoso *et al*., 2016; Cardoso *et al*., 2019; Lucinda, 2008; Mariguela *et al*., 2013; Souza *et al*., 2018). Recent cytogenetic studies indicated the existence of cryptic species within *Hypostomus* cf. *wuchereri* (Günther, 1864) and *Hypostomus ancistroides* (Ihering, 1911) (Bitencourt *et al*., 2011; Endo *et al*., 2012), whereas analyses of genomic data from double-digest restriction site-associated DNA sequencing (ddRAD-seq) strongly supported the existence of six distinct clades of *Hypostomus* in headwater streams of the Distrito Federal region (Bagley *et al*., 2021). Taxonomic assessment and description of these new species/lineages of *Hypostomus* would be of great importance for facilitating their inclusion in regional to national fisheries management and conservation programmes. In addition, if these species/lineages proved morphologically diagnosable, then clarifying their geographical distributions and giving them formal taxonomic names would provide foundational knowledge for future studies adding to the understanding of their ecology and evolution (Bickford *et al*., 2007; Delic *et al*., 2017). This study presents the findings of morphological analyses testing the hypothesis that two new candidate species of *Hypostomus* from central Brazil discovered in genome-wide phylogeographical analyses by Bagley *et al*. (2021), known as *Hypostomus* sp. 2 clade 3 and *Hypostomus* sp. 2 clade 6, are morphologically distinct. It is shown that these lineages indeed represent two new species, which are described here. Using modern machine learning techniques, diagnostic features are identified in the morphology of these species.

2 | MATERIALS AND METHODS

2.1 | Material examined

This study examined 701 *Hypostomus* specimens from 44 described species and putative candidate species (Supporting Information Appendix S1), including specimens already present in natural history collections, as well as new material obtained by conducting field sampling using 3 × 1 m seines with 2 mm mesh diameter. Wherever possible, at least 10 individual specimens of each new species described here were deposited in the following collections: Coleção de Peixes da Universidade Federal de Mato Grosso (CPUFMT); Coleção de Peixes do Departamento de Zoologia e Botânica do Instituto de Biociências, Letras e Ciências Exatas, Universidade Estadual Paulista, São José do Rio Preto (DZSJRP); Coleção Ictiológica da Universidade de Brasília (CIUNB); Coleção Ictiológica do Núcleo de Pesquisas em Limnologia, Ictiologia e Aquicultura, Universidade Estadual de Maringá (NUP); Coleção Zoológica da Universidade Federal de Mato Grosso do Sul (ZUFMS); Departamento de Zoologia, Universidade Federal do Rio Grande do Sul (UFRGS); Laboratório de Biologia e Genética de Peixes, Universidade Estadual Paulista, Botucatu (LBP); Museu de Ciências e Tecnologia, Pontifícia Universidade Católica do Rio Grande do Sul (MCP); Museu de Zoologia da Universidade de São Paulo (MZUSP); Museu de Zoologia da Universidade Estadual de Londrina (MZUEL); Museu Nacional, Universidade Federal do Rio de Janeiro (MNRJ); and Universidade Federal do Tocantins, Porto Nacional (UNT). In this work, for comparative purposes, the super-groups identified and proposed by Jardim de Queiroz *et al*. (2020) were used, because many of the species examined here were included in their super-groups (including *H. cochliodon*, *H. auroguttatus* and *H. plecostomus*). For more details, refer to the list of material examined in this study in Supporting Information Appendix S1.

2.2 | Ethical statement

Sampling activities performed to obtain new specimens during the course of this study were executed in accordance with Brazilian law and with permission from the Sistema de Autorização e Informação em Biodiversidade (SISBIO; permit no. 63008-1) of the Instituto Chico Mendes de Conservação da Biodiversidade (ICMBio) and the Comitê de Ética de Uso Animal of the Universidade de Brasília (CEUA-UnB, protocol no. 52/2018). After sampling, the animals were euthanized by eugenol immersion (Griffiths, 2000), fixed in 10% formaldehyde, preserved in 70% ethanol (Uieda & Castro, 1999) and deposited in the CIUNB.

2.3 | Morphological data

This study investigated the variation in 41 morphological characters, comprising 8 meristic characters, 29 quantitative (measurement) characters and 4 qualitative characters. Bilaterally symmetrical morphological characters were measured or scored, whenever possible, from the left side of the examined specimens. Based on nomenclature in Schaefer (1997) and Oyakawa *et al*. (2005), the numbers of lateral line plates, predorsal plates, dorsal-fin base plates, plates between dorsal fin and adipose fin, plates between adipose fin and caudal fin, ventral plates between anal fin and caudal fin, teeth of the premaxillary and dentary of each specimen were counted. In addition, following the nomenclature and methods of Boeseman (1968) modified by Weber (1985) and Zawadzki *et al*. (2017b), the following measurements were recorded: standard length (SL), axial length, total length, predorsal length, pre-anal length, head length, interdorsal length, thoracic length, abdominal length, caudal peduncle length, caudal peduncle depth, first dorsal-fin ray length, dorsal-fin base length, first pectoral-fin ray length, first pelvic-fin ray length, upper caudal-fin ray length, lower caudal-fin ray length, spine length adipose fin, cleithral width, head depth, body depth at dorsal-fin base, snout length, interorbital width, orbital diameter, anal-fin ray length, premaxillary ramus length, dentary ramus length, maxillary barbel length, lower lip width and lower lip length. All measurements were taken point to point using digital callipers accurate to within ±0.1 mm. Qualitative categorical data on the presence or absence of plate keels, presence of plates on the abdomen, presence of plates in the cleithrum region and colour pattern were also collected.

2.4 | Statistical analysis

To minimize scale effects and non-normality, all linear morphological variables were log-transformed. Size-free data variables were then obtained for use in downstream multivariate analyses by combining methods reviewed by Rohlf and Bookstein (1987). Body size was defined as an isometric size variable using the method of Somers (1986). Next, scores of an isometric eigenvector were calculated, which is defined *a priori* as $p^{-0.5}$ (where p is the number of data variables), by multiplying the $n \times p$ matrix of log-transformed data by the $p \times 1$ isometric eigenvector (Jolicouer, 1963; Somers, 1986). To remove body size effects contained in the log-transformed data, the method of Burnaby (1966) was applied, which consists of multiplying the log-transformed $n \times p$ data matrix by a $p \times p$ symmetric matrix, L, defined as

$$L = I_p - V\left(V^T V\right)^{-1} - V^T$$

where I_p is the $p \times p$ identity matrix, V is the isometric eigenvector defined previously and held constant and V^t is the transposed form of V (Rohlf & Bookstein, 1987).

Several analyses of the final, size-free shape variables obtained earlier were conducted to test for morphological differences between the *Hypostomus* species and candidate species examined in Supporting Information Appendix S1. First, the data for outliers were inspected. To identify possible univariate outliers, boxplot graphs were checked "by-eye." To identify multivariate outliers, checks were conducted using the CovNAClassic (Classical Estimates of Multivariate Location and Scatter for incomplete data) approach, as well as a robust method based on Mahalanobis distance that can be used when some observations are missing (*missing data*, NAs), as implemented in the RRCOVNA R package (Todorov, 2016). Outlier tests were conducted using a stringent significance level of $\alpha = 0.001$. When the outliers were determined to have resulted from typos or erroneous measurements, every effort was made to correct them when possible; otherwise, the outlier observations were replaced with scores of "NA."

Missing values, *e.g*., caused by broken fin rays or broken or missing teeth in a given fish specimen, are undesirable in multivariate analyses of morphological data sets, as they require the removal of the entire set of recorded observations from each individual with missing data, and can result in substantial data loss. Thus, missing values were replaced with estimated values imputed using the random forest (RF) approach implemented in the MISSFOREST R package (Stekhoven & Buhlmann, 2012). This method is advantageous because it imputes both categorical and continuous data simultaneously while also estimating the imputation error rate (Stekhoven & Buhlmann, 2012).

To select the best morphological predictors of the species limits, guided regularized random forest (GRRF) (Deng & Runger, 2013) as implemented in the R packages, RANDOMFOREST (Liaw & Wiener, 2002), and regularized random forest (RRF) were used (Deng, 2013). The GRRF approach is a variation of the RF, a machine-learning classification method which combines predictions from multiple decision trees based on a random sub-set of predictors and data (Breiman, 2001). Under the GRRF approach, importance scores (contributions of each predictor) from an ordinary RF generated through a run on a complete training data set are used to guide an RRF predictor selection method, allowing the user to select better predictors when multiple predictors share the same maximal information gain (Deng & Runger, 2013). During the RRF component of the procedure, regularization penalizes the selection of new predictors for the split of observations during the construction of RF decision trees when the information gain (*i.e*., the decrease in Gini impurity) is similar to that obtained with previously used predictors. Machine learning algorithms such as GRRF have proven effective for identifying diagnostic characters in recent papers in systematics (Breitman *et al*., 2018; Murphy *et al*., 2016). As a result, two GRRF analyses were performed for *Hypostomus* sp. 2 clade 3, including comparisons (1) against all other species and (2) against only *Hypostomus* sp. 2 clade 6. To round out the analysis, GRRF for *Hypostomus* sp. 2 clade 6 was performed when compared against all other species. In each analysis, 1000 decision trees were grown, and the default RRF package settings were used (Deng, 2013), maintaining predictors such that the average decrease in Gini impurity was greater

than one; 100 tenfold cross-validation repetitions were also used sequentially increasing the number of predictors to evaluate the accuracy of the GRRF models. All statistical analyses were performed using R v5.0 (R Core Team, 2018).

3 | RESULTS

In the comparisons among *Hypostomus* sp. 2 clade 3 and all other grouped species, the full GRRF model showed high accuracy, with an average cross-validation error rate of only 0.03 (Figure 1a). In descending order of importance, the GRRF analysis selected size-corrected versions of the following morphological variables as the best predictors differentiating *Hypostomus* sp. 2 clade 3 from all other species: caudal peduncle depth, first pectoral-fin ray length, dorsal-fin base length, cleithral width, thoracic length, head length, first dorsal-fin ray length and orbit diameter (Figure 1b). Re-running GRRF while including only these eight best predictors also yielded a model with an average cross-validation error rate of 0.03. *Hypostomus* sp. 2 clade 3 has the largest values for caudal peduncle depth, the smallest values for the first pectoral-fin ray length and dorsal-fin base length, the narrowest cleithral width, the shortest thoracic length, the longest head, the shortest first ray of the dorsal fin and a smaller orbit than the other species examined (Table 1; Figure 1c,d).

In the comparison of morphological variation between *Hypostomus* sp. 2 clade 3 and *Hypostomus* sp. 2 clade 6, the full GRRF model showed high accuracy, with an average cross-validation error rate of only 0.04 (Supporting Information Figure S1A). In descending order of importance, GRRF analysis selected caudal peduncle depth, first pectoral-fin ray length, body size, dorsal-fin base length, lateral line plate series, caudal-fin ray length, lower lip length and thoracic length as the best predictors for differentiating *Hypostomus* sp. 2 clades 3 and

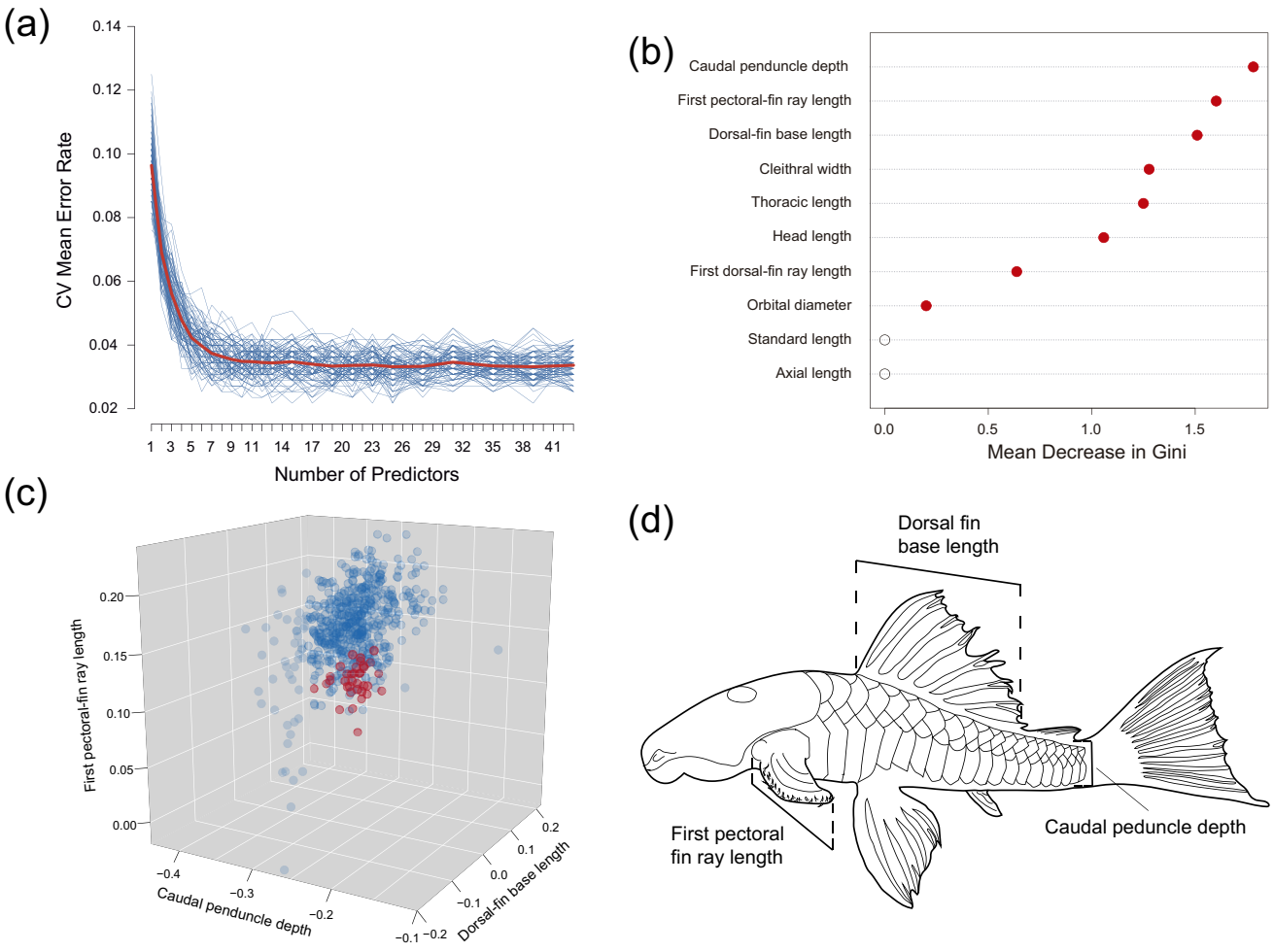

FIGURE 1 Guided regularized random forest (GRRF) analysis of morphological data for prediction of *Hypostomus cafuringa vs*. all other species of *Hypostomus* examined. (a) Prediction error with an increasing number of predictors ranked by importance, based on 100 replicates of 10-fold cross-validation. Blue lines indicate the error rate for each replicate; the red line indicates the mean error rate. (b) Ten most important morphological predictors based on mean decrease in model accuracy, as measured by Gini impurity; best predictors indicated by red circles. (c) Variation in caudal peduncle depth, first pectoral-fin ray length and dorsal-fin base length, the three best predictors of *H. cafuringa vs*. all other *Hypostomus* species examined. (d) Schematic drawing of *Hypostomus*, indicating the same three best predictors. ● *Hypostomus cafuringa*; ● all examined species of *Hypostomus*

TABLE 1 Most informative morphometric and meristic characters to diagnose species of *Hypostomus*

Characters	*Hypostomus cafuringa*	*Hypostomus crulsi*	Species examined[a]
Axial length	0.74–0.84 (0.76 ± 0.01)	0.76–0.91 (0.80 ± 0.05)	0.67–0.85 (0.77 ± 0.02)
Body size	3.30–6.88 (5.94 ± 0.65)	2.79–6.22 (4.41 ± 1.28)	3.19–9.02 (6.93 ± 1.13)
Head length	0.22–0.32 (0.24 ± 0.01)	0.11–0.30 (0.23 ± 0.04)	0.07–0.27 (0.22 ± 0.02)
Thoracic length	−0.03–0.06 (0.02 ± 0.02)	−0.02–0.11 (0.04 ± 0.03)	−0.03–0.17 (0.06 ± 0.03)
Abdominal length	−0.06–0.04 (−0.01 ± 0.02)	−0.19–0.11 (−0.07 ± 0.05)	−0.25–0.10 (−0.01 ± 0.03)
Caudal peduncle depth	−0.33–0.25 (−0.28 ± 0.01)	−0.37–0.26 (−0.33 ± 0.02)	−0.43–0.21 (−0.31 ± 0.03)
First dorsal-fin ray length	0.01–0.11 (0.06 ± 0.02)	−0.01–0.09 (0.05 ± 0.03)	−0.07–0.33 (0.14 ± 0.04)
Dorsal-fin base length	−0.02–0.07 (0.03 ± 0.02)	−0.19–0.10 (0.01 ± 0.08)	−0.08–0.21 (0.09 ± 0.04)
First pectoral-fin ray length	0.07–0.13 (0.10 ± 0.01)	−0.01 – 0.13 (0.07 ± 0.05)	0.03–0.23 (0.15 ± 0.02)
First pelvic-fin ray length	0.02–0.09 (0.05 ± 0.01)	−0.04–0.11 (0.05 ± 0.05)	−0.01–0.18 (0.08 ± 0.02)
Upper caudal-fin ray length	0.03–0.19 (0.09 ± 0.02)	0.07–0.28 (0.15 ± 0.06)	−0.21–0.28 (0.12 ± 0.05)
Lower caudal-fin ray length	0.09–0.29 (0.14 ± 0.03)	0.12–0.39 (0.24 ± 0.08)	0.01–0.31 (0.17 ± 0.05)
Cleithral width	0.16–0.19 (0.17 ± 0.01)	0.12–0.20 (0.17 ± 0.02)	0.06–0.24 (0.17 ± 0.02)
Orbital diameter	−0.52–0.38 (−0.46 ± 0.32)	−0.60–0.46 (−0.51 ± 0.03)	−0.72–0.35 (−0.52 ± 0.07)
Lower lip length	−0.69–0.47 (−0.60 ± 0.04)	−0.60–0.36 (−0.48 ± 0.07)	−0.91–0.29 (−0.65 ± 0.08)
Median plate series	25–27 (26 ± 0.54)	24–26 (25 ± 0.26)	24–30 (26 ± 1.18)

Notes. Values represent minimum, maximum and mean ± S.D. in parentheses. Body size represents isometric size, whereas the remaining morphometric variables are size-adjusted. See the text for details.

[a]Variables of all species examined, except *H. cafuringa* and *H. crulsi*.

6 (Supporting Information Figure S1B). A GRRF model based on these eight predictors had an average cross-validation error rate of 0.12 (Supporting Information Figure S1A). Relative to *Hypostomus* sp. 2 clade 6, it is observed that *Hypostomus* sp. 2 clade 3 has a higher caudal peduncle, longer pectoral-fin first ray, larger body size, longer dorsal-fin base, a greater series of lateral line plate lines, shorter caudal-fin ray, shorter lower lip and shorter thoracic length (Table 1; Supporting Information Figures S1C and S1D).

In the comparison of *Hypostomus* sp. 2 clade 6 with all other species combined, the full GRRF model showed slightly higher accuracy, with an average cross-validation error rate of only 0.02 (Figure 2a). The GRRF analysis selected first pelvic-fin ray length, first pectoral-fin first ray length, isometric size, lower lip length, dorsal-fin base length and axial length as the best predictors for differentiating *Hypostomus* sp. 2 clade 6 from all other species examined (Figure 2b). A GRRF model based only on these six best predictors also had an average cross-validation error rate of 0.02 (Figure 2a). *Hypostomus* sp. 2 clade 6 has a shorter first ray of the pelvic fin, shorter first ray of the pectoral fin, smaller body size, shorter lower lip, shorter dorsal-fin base and the longest axial length (Table 1; Figure 2c,d).

Considering these quantitative morphological differences among the candidate species formed by *Hypostomus* sp. 2 clades 3 and 6 in Bagley *et al*. (2021) and other *Hypostomus* species from the region, formal descriptions of these lineages are provided next as the new species *H. cafuringa* and *Hypostomus crulsi*, respectively.

4 | *HYPOSTOMUS CAFURINGA*, NEW SPECIES

urn:lsid:zoobank.org:act:4454562E-9EA3-4F0C-9C3B-D35A1511646F

(Figures 3-4 and Tables 1-2)

Hypostomus sp. 2 (Aquino & Colli, 2017).

Hypostomus sp. 2 clade 3 (Bagley *et al*., 2021).

4.1 | Holotype

CIUNB 1489; 77.28 mm SL; Brazil, Distrito Federal, Brasília, Fercal, upper Tocantins River basin, tributary of rio Maranhão, ribeirão Contagem near the bridge, 15.5916666667 S, 47.8858333333 W, 850 m a.s.l., 20 November 2018, Y. F. F. Soares, G. O. Cunha, L. F. G. O. Yung, M. R. R. Junior and L. Damásio.

4.2 | Paratypes

All from Brazil, Distrito Federal, upper Tocantins River basin. CIUNB 1490 (2, 55.67–75.66 mm SL), 01 August 2018, P. P. U Aquino, Y. F. F. Soares and L. P. C. Machado, same as holotype location. CIUNB 1491 (1, 42.42 mm SL), 13 March 2015, P. P. U. Aquino and J. C. Bagley, same as holotype location. CIUNB 1492 (12, 50.36–77.28 mm SL), 20 November 2018, Y. F. F. Soares, G. O. Cunha, L. F. G. O. Yung, M. R. R. Junior and L. Damásio, same as holotype location. CIUNB

1493 (1, 66.96 mm SL); Brasília, ribeirão Cafuringa near the bridge, border between the Brazilian states of Goiás and Distrito Federal, −15.5016666667 S, −47.9763888889 W, 1 August 2018, P. P. U. Aquino, Y. F. F. Soares and L. P. C. Machado. CIUNB 1494 (3, 73.19–89.62 mm SL); Brasília, Fercal, ribeirão Engenho Velho, −15.5894444444 S, −47.8755555556 W, 4 December 2018, A. G. T. Cardoso. CIUNB 1495 (4, 34.85–64.44 mm SL); Brasília, Fercal ribeirão do Buraco, −15.6016666667 S, −47.9111111111 W, 13 March 2015, P. P. U. Aquino and J. C. Bagley. CIUNB 1496 (1, 18.62 mm SL); Brasília, ribeirão Cafuringa near the bridge, border between the Brazilian states of Goiás and Distrito Federal, −15.5016666667 S, −47.9763888889 W, 9 March 2015, P. P. U. Aquino and J. C. Bagley. DZSJRP 23118 (4, 55.57–74.07 mm SL), 20 November 2018, Y. F. F. Soares, G. O. Cunha, L. F. G. O. Yung, M. R. R. Junior and L. Damásio, same as holotype location. MNRJ 52557 (4, 65.20–72.10 mm SL), 20 November 2018, Y. F. F. Soares, G. O. Cunha, L. F. G. O. Yung, M. R. R. Junior and L. Damásio, same as holotype location. MZUSP 125831 (2, 56.10–61.90 mm SL), 1 August 2018, P. P. U Aquino, Y. F. F. Soares and L. P. C. Machado, same as holotype location.

4.3 | Diagnosis

H. cafuringa is distinguished from the species of *H. cochliodon* super-group by slender viliform bicuspid teeth (*vs*. robust spoon-shaped teeth) and by dentary and premaxillary branch angles greater than 90° (*vs*. angles up to 90°); it is distinguished from the remaining congeners of *H. auroguttatus* super-group by the small size of the premaxillary and dentary, with low number of teeth (22–49, mean 38) [*vs*. large size of the premaxillary and dentary, with high number of teeth (20–140, mean 60)]. The new species is distinguished from the *H. plecostomus* super-group by an abdominal area partially covered by platelets, forming a triangle (*vs*. abdominal area completely plated), and by the absence of developed rows of

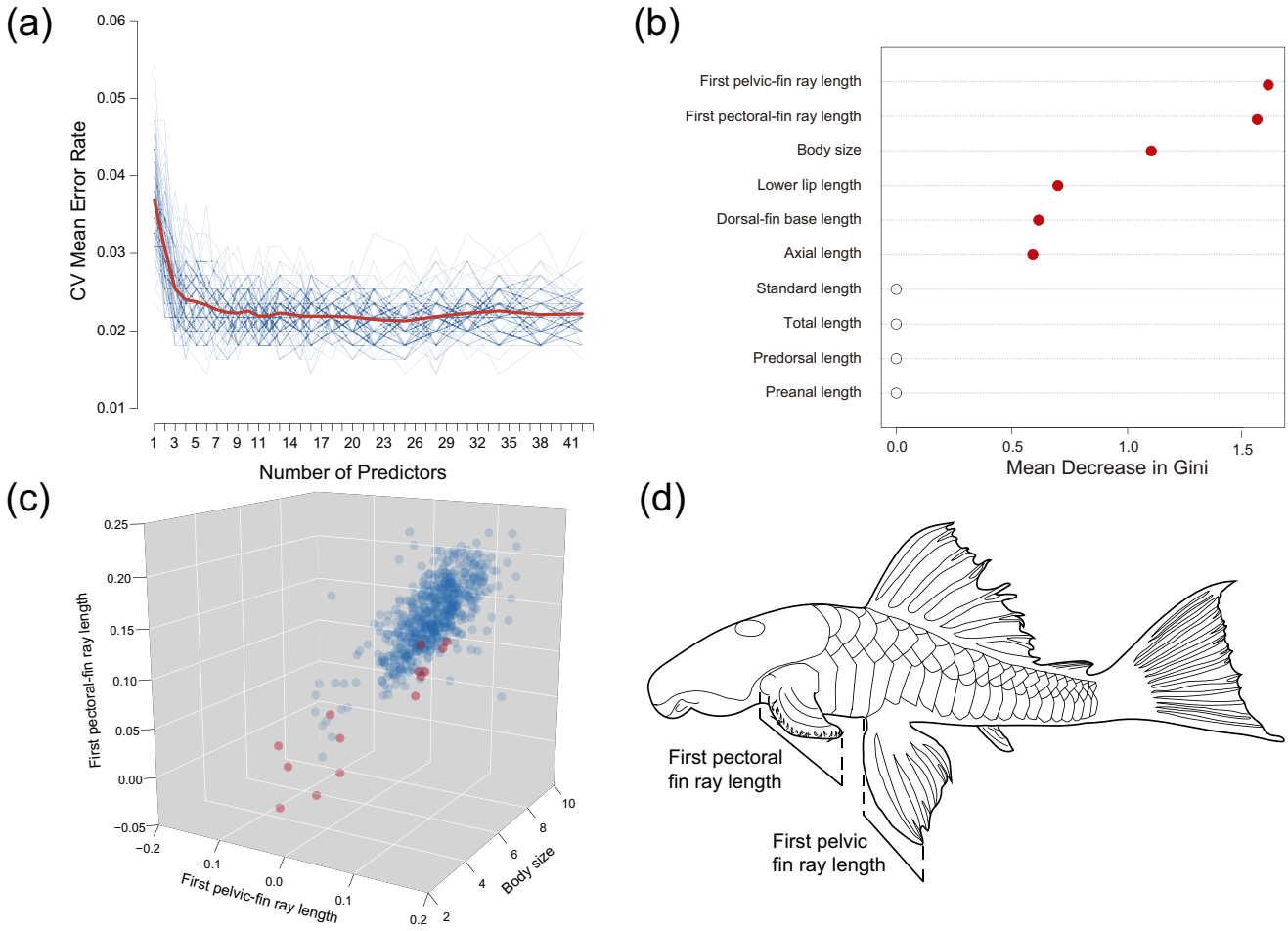

FIGURE 2 Guided regularized random forest (GRRF) analysis of morphological data for prediction of *Hypostomus crulsi vs*. all other species of *Hypostomus* examined. (a) Prediction error with an increasing number of predictors ranked by importance, based on 100 replicates of 10-fold cross-validation. Blue lines indicate the error rate for each replicate; the red line indicates the mean error rate. (b) Ten most important morphological predictors based on mean decrease in model accuracy, as measured by Gini impurity; best predictors are indicated by red circles. (c) Variation in pelvic-fin first ray length, first pectoral-fin ray length and isometric size, the three best predictors of *H. crulsi vs*. all other *Hypostomus* species examined. (d) Schematic drawing of *Hypostomus*, indicating the two best linear predictors (body size is a linear combination of all body measurements). ● *Hypostomus crulsi*; ● all examined species of *Hypostomus*

odontodes on keels (*vs.* moderate to well-developed rows of odontodes on keels). In addition, among other species in the *H. auroguttatus* supergroup, *H. cafuringa* can be distinguished from *Hypostomus nigrolineatus*, *Hypostomus subcarinatus* and *H. delimai* by the absence of well-developed rows of odontodes on keels (*vs.* moderate to well-developed row of odontodes on keels); from *Hypostomus alatus* and *Hypostomus tietensis* by dark spots on a light background (*vs.* light spots on a dark background); from *H. denticulatus* and *Hypostomus kuarup* by the small number of teeth in the premaxillary and dentary (22–49) [*vs.* large number of teeth in the premaxillary and dentary (60–205)]; from *Hypostomus garmani*, *Hypostomus latirostris* and *Hypostomus macrops* by the diameter of the spots distributed on the body, smaller than or equal to the diameter of the pupil (*vs.* spots approximately equal to or greater than the diameter of the pupil); from *Hypostomus lima* by the shorter first dorsal-fin ray length (21.2%–27.5% in SL) (*vs.* 28%–32.95% in SL) and by larger cleithral width (30.2–34.1 in SL, mean 31.6) (*vs.* 27.1–31.5 in SL, mean 29.9).

TABLE 2 Morphometric and meristic data of *Hypostomus cafuringa*

	Holotype	Range	Mean ± S.D.
Total length (mm)	102.5	29.8–117.1	
Standard length (mm)	77.2	18.2–89.6	
Percentage of standard length			
Head length	35.5	34.9–47.7	37.0 ± 2.1
Predorsal length	42.8	42.2–47.8	44.2 ± 1.2
Interdorsal length	12.5	7.2–15.4	12.8 ± 1.6
Pre-anal length	66.4	63.7–68.2	66.2 ± 1.0
Thoracic length	21.6	20.1–24.3	22.2 ± 0.9
Abdominal length	22.0	18.1–22.3	20.4 ± 1.0
Caudal peduncle length	30.1	28.6–36.7	30.7 ± 1.8
Caudal peduncle depth	10.7	9.4–12.1	10.9 ± 0.5
First dorsal-fin ray length	23.8	21.2–27.5	24.6 ± 1.6
Dorsal-fin base length	23.4	21.1–25.1	22.9 ± 1.0
Anal-fin spine length	10.6	8.9–13.1	10.9 ± 0.8
First pectoral-fin ray length	27.3	24.5–29.5	27.0 ± 1.2
First pelvic-fin ray length	23.5	22.2–27.5	24.0 ± 1.3
Upper caudal-fin ray length	23.9	22.2–34.5	26.3 ± 2.2
Lower caudal-fin ray length	27.0	25.2–43.7	29.2 ± 3.4
Adipose-fin spine length	7.5	6.8–11.5	8.4 ± 1.0
Body depth at dorsal-fin base	20.4	19.9–24.2	21.6 ± 1.1
Cleithral width	30.4	30.2–34.1	31.6 ± 1.0
Percentage of head length			
Head depth	54.3	43.4–59.6	53.4 ± 3.0
Snout length	58.3	45.2–63.3	58.2 ± 3.8
Orbital diameter	16.9	15.7–23.3	19.5 ± 1.5
Interorbital width	33.9	28.0–39.0	32.9 ± 2.1
Mouth width	61.7	45.9–65.0	58.1 ± 4.1
Dentary ramus length	21.7	16.8–23.1	20.5 ± 1.5
Premaxillary ramus length	21.4	24.2–34.4	29.6 ± 2.3
Maxillary barbel length	4.9	4.9–10.7	8.6 ± 1.3
Meristic counts			Mode
Median plates series	26	25–27	26
Predorsal plates	3	3–4	3
Dorsal plates below dorsa-fin base	9	7–9	8
Plates between dorsal and adipose fin	4	4–5	5
Plates between adipose and caudal fin	4	3–4	4
Plates between end of anal-fin base and caudal fin	13	11–13	12
Premaxillary teeth	49	27–49	42
Dentary teeth	45	22–47	34

Finally, *H. cafuringa* can be distinguished from *H. crulsi* by abdominal area partially covered with triangle-shaped platelets (*vs.* naked abdominal area).

4.4 | Description

Morphometric and meristic data are provided in Table 2. Largest SL 89.62 mm. Highest body depth at origin of dorsal fin. Largest body width at cleithral region, tapering progressively towards caudal peduncle; cleithral width greater than head depth.

Dorsal profile slightly convex from snout tip to origin of dorsal fin; slightly concave from origin of dorsal fin to end of caudal peduncle; rising again near caudal-fin insertion. Ventral profile of body almost straight from snout tip to origin of pelvic fin; postero-dorsally inclined from origin of pelvic fin to origin of anal fin. Ellipsoid-shaped caudal peduncle in cross-section.

Slightly depressed head, moderately broad and with rounded snout in dorsal view. Mesethmoid forming a light, rounded crest from tip of snout to region between nostrils. Slightly accented lateral crested head from nostrils to posterior margin of compound pterotic; poorly developed in front of posterorbital region and along compound pterotic. Posterior process of parieto-supraoccipital delimited by triple or quadruple predorsal plate in some specimens. Axis-shaped operculum with small and undeveloped odontodes. Slightly noticeable facial plates with small odontodes. Eyes dorsolateral, with diameter 15.7%–23.2% of head length. Moderately sized round oral disc. Outer edge of the upper lip without plates, but with small odontodes forming lateral lines in the anterior region of the lip. Maxillary barbel slightly smaller than eye diameter, attached to lip in proximal region, without ornamentation. Premaxillary teeth 28–49; dentary teeth 26–47. Dentary branches short, forming an angle of *c.* 140–155° to each other. Bicuspid thin teeth curved inward distally; lanceolate, medial cusp considerably larger than pointed lateral cusp. Teeth crown bent ventrally.

Snout tip dorsally covered by small plates and odontodes, completely naked at anteroventral portion. Ventral surface of head naked, except for small groups of plates above transverse line through gill openings. Five lateral plate series: dorsal series with 7–9 plates (mode 8), limiting naked area along base of dorsal fin; mid-dorsal series with 23–24 plates (mode 24); median series with 25–27 (mode 26) perforated plates; mid-ventral series with 24–25 (mode 24) plates; ventral series with 19–22 (mode 21) plates, starting at insertion of pelvic fin or slightly previous; two to three ventral plates along base of anal fin, and 11–13 (mode 12) ventral plates from that point to caudal fin. Dorsal, mid-dorsal and mid-ventral plate series without conspicuous longitudinal keels. Abdomen partially covered by plates distributed mainly along shoulder girdle and central portion of abdomen triangle shaped. Larger individuals with larger areas covered with plates, except laterally in abdomen, always naked.

Dorsal fin II, 7; moderate size; flexible thorn, its distal border almost straight to slightly convex, not reaching the adipose fin when adpressed. Adipose-fin spine well developed, usually straight, its distal tip depressed and not reaching upper caudal-fin ray. Pectoral fin I, 6; distal border straight. Pectoral spine slightly curved, with rounded tip and generally with inwardly curved and slightly hypertrophied odontodes, concentrated in distal portion in larger individuals. Pectoral spine reaching beyond pelvic-fin insertion. Pelvic fin i, 5, and with slightly rounded distal border. The unbranched pelvic-fin ray curved inward, surpassing origin of unbranched ray of anal fin when adpressed Anal fin i, 4; distal tip of posterior rays reaching fifth or sixth plate posterior to origin of adpressed anal fin. Caudal fin i, 7 + 7, i; with moderately strong unbranched rays and lower lobe larger than upper lobe.

4.5 | Colour in alcohol

Colour of dorsal and lateral surfaces of the head and trunk homogeneous brown or grey (Figure 3). Head covered by conspicuous dark

FIGURE 3 *Hypostomus cafuringa*, CIUNB 1489, holotype, standard length 77.3 mm; Brazil: Distrito Federal: Ribeirão da Contagem, upper Tocantins river basin

FIGURE 4 Live specimen of *Hypostomus cafuringa*, CIUNB 1490, 75.7 mm in standard length, paratype, Distrito Federal: Ribeirão da Contagem, upper Tocantins river basin

spots, not forming a smudge pattern; diameter less than or equal to pupil diameter. Body usually with conspicuous dark spots, larger than those found on head; spots evenly observed along trunk of individuals. Fins light brown to greyish in colour. Dorsal fin with dark spots, distinctly larger than those on head and body; spots usually distributed serially on each interradial membrane. Caudal fin with light to greyish brown colour with conspicuous dark spots usually arranged in bars. Dorsal and adipose fins with conspicuous spots forming transverse bars.

4.6 | Colour in life

Description based on field observations of various specimens and images of living specimens (Figure 4). General body colour light brown or brown. Conspicuous, round black spots on body, fins and radial membranes similar to specimens preserved in alcohol. Ventral surface of head and abdomen light brown without dark spots.

4.7 | Geographic distribution

The new species is known only from the headwater streams of the Maranhão River, a tributary of the Tocantins River, in the upper Tocantins River basin, central Brazil (Figure 5).

4.8 | Natural history

H. cafuringa specimens were captured in headwater streams of the Maranhão River, in 4–7 m wide and 0.4–1.0 m deep sections, with rocky bottom and gravel, transparent water, medium-to-fast water current and very high and rugged relief with altitudes ranging from 783 to 897 m a.s.l. The riparian vegetation of these streams is mostly dense, inserted within the Cerrado (Brazilian savanna). The sampled areas are located in the Cafuringa Environmental Protection Area (EPA), which is recognized as an area of ecological interest for conservation that allows human occupation and land use in an orderly and sustainable manner. In any case, the points sampled are in regions of great human influence (*e.g.*, with urban sprawl, pollution and exploitation of mineral resources). *H. cafuringa* was predominantly associated with rocky sections and fast-flowing water, which can make sampling difficult if the rocks are not overturned.

Specimens of *H. cafuringa* co-occur with *Ancistrus aguaboensis* Fisch-Muller, Mazzoni and Weber, 2001, *Apareiodon machrisi* Travassos, 1909, *Geophagus brasiliensis* (Quoy and Gaimard, 1824), *Harttia punctata* Rapp Py-Daniel and Oliveira, 2001, *Hypostomus* cf. *plecostomus* (Linnaeus, 1758), *Imparfinis borodini* Mees and Cala, 1989, *Knodus chapadae* (Fowler, 1906), *Moenkhausia* cf. *aurantia* Bertaco, Jerep and Carvalho, 2011, and *Phenacorhamdia somnians* (Mees, 1974). It is also found with invasive species such as *Poecilia*

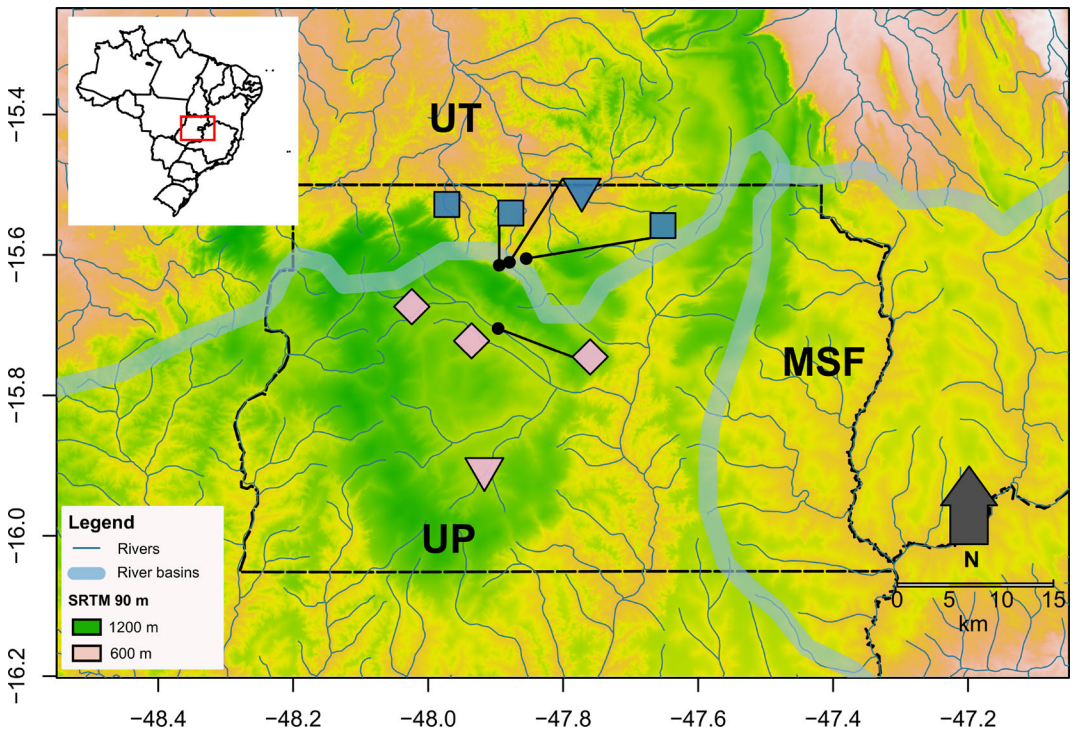

FIGURE 5 Distribution of *Hypostomus cafuringa* (blue symbols) and *Hypostomus crulsi* (pink symbols). Triangles represent the respective type localities. UP: upper Paraná basin, UT: upper Tocantins basin, MSF: middle São Francisco basin. Elevation based on the Shuttle Radar Topographic Mission (SRTM) 90 m Digital Elevation Database

reticulata Peters, 1859, which are abundant near areas with human settlements and agricultural disturbances.

4.9 | Etymology

The specific epithet *cafuringa* refers to the Cafuringa EPA and the Cafuringa stream where the species is found; a noun in apposition.

5 | *HYPOSTOMUS CRULSI*, NEW SPECIES

urn:lsid:zoobank.org:act:135779C5-46C1-4567-B368-DAD2040FC134

(Figures 6-7 and Tables 1, 3)

Hypostomus sp. 2 (Aquino *et al*., 2009; Aquino & Couto, 2010; Aquino & Colli, 2017).

Hypostomus sp. 2 clade 6: (Bagley *et al*., 2021).

TABLE 3 Morphometric and meristic data of *Hypostomus crulsi*

	Holotype	Range	Mean ± S.D.
Total length (mm)	83.9	28.9–112.7	
Standard length (mm)	62.3	16.8–82.9	
Percentage of standard length			
Head length	34.2	24.5–41.3	36.0 ± 4.1
Predorsal length	42.6	34.5–48.6	44.2 ± 3.1
Interdorsal length	15.3	8.7–48.6	12.4 ± 2.7
Pre-anal length	66.7	52.8–69.6	66.0 ± 4.0
Thoracic length	23.9	17.5–27.4	23.2 ± 2.3
Abdominal length	19.9	11.9–22.0	18.2 ± 2.6
Caudal peduncle length	30.3	26.5–33.6	30.9 ± 1.8
Caudal peduncle depth	9.9	8.6–10.14	9.6 ± 0.4
First dorsal-fin ray length	25.3	20.8–27.1	23.7 ± 1.8
Dorsal-fin base length	25.1	17.0–25.8	21.7 ± 3.8
Anal-fin spine length	10.9	8.3–12.5	10.5 ± 1.1
First pectoral-fin ray length	27.9	17.8–29.4	25.1 ± 3.3
First pelvic-fin ray length	27.0	17.2–28.5	23.8 ± 3.3
Upper caudal-fin ray length	25.9	24.4–35.9	29.4 ± 4.0
Lower caudal-fin ray length	30.4	28.3–47.0	36.0 ± 6.7
Adipose-fin spine length	8.0	6.3–10.0	8.1 ± 1.2
Body depth at dorsal-fin base	20.9	17.0–22.2	20.1 ± 1.6
Cleithral width	30.8	27.9–34.2	31.2 ± 1.7
Percentage of head length			
Head depth	61.3	46.5–63.5	56.8 ± 9.8
Snout length	60.0	44.5–61.7	54.5 ± 5.3
Orbital diameter	15.2	14.8–25.0	17.8 ± 2.4
Interorbital width	35.0	31.7–42.2	34.7 ± 3.2
Mouth width	58.9	39.7–66.7	57.5 ± 7.0
Dentary ramus length	19.2	14.7–28.3	19.6 ± 3.1
Premaxillary ramus length	20.4	14.0–26.2	19.3 ± 3.2
Maxillary barbel length	11.0	8.8–16.8	11.3 ± 2.0
Counts			Mode
Median plates series	25	24–26	25
Predorsal plates	3	3	3
Dorsal plates below dorsa-fin base	8	7–8	8
Plates between dorsal and adipose fin	5	4–5	5
Plates between adipose and caudal fin	4	3–4	4
Plates between end of anal-fin base and caudal fin	12	11–12	12
Premaxillary teeth	44	25–46	35
Dentary teeth	37	20–42	31

5.1 | Holotype

CIUNB 1497; 61.25 mm SL; Brazil, Distrito Federal, Brasília, upper Paraná River basin, Paranaíba River drainage, tributary of rio São Bartolomeu, ribeirão Taquara, Fazenda Água Limpa da Universidade de Brasília (FAL – UnB), −15.9105555556 S, −47.9088888889 W, 1035 m a.s.l.; 5 March 2015, P. P. U. Aquino and J. C. Bagley.

5.2 | Paratypes

All from Brazil, Distrito Federal, upper Paraná River basin. CIUNB 1498 (1, 25.11 mm SL), 5 March 2015, P. P. U. Aquino and J. C. Bagley, same as holotype location. CIUNB 1499 (1, 44.73 mm SL), Brasília, córrego Milho Cozido, Parque Nacional de Brasília (PNB), −15.6669444444 S, −48.0188888889 W, 6 March 2015, P. P. U. Aquino and J. C. Bagley. CIUNB 1500 (1, 17.32 mm SL), Brasília, ribeirão Bananal, Parque Nacional de Brasília (PNB), −15.7319444444 S, −47.9122222222 W, 6 March 2015, P. P. U. Aquino and J. C. Bagley. CIUNB 1501 (6, 16.82–52.82 mm SL), Brasília, ribeirão do Torto, −15.6997222222 S, −47.9058333333 W, 6 March 2015, P. P. U. Aquino and J. C. Bagley. CIUNB 599 (1, 52.62 mm SL), Brasília, córrego Milho Cozido, Parque Nacional de Brasília (PNB), −15.6669444444 S, −48.0188888889 W, 8 October 2010, P. P. U. Aquino. CIUNB 915 (2, 44.28–65.24 mm SL), Brasília, córrego Milho Cozido, Parque Nacional de Brasília (PNB), −15.6669444444 S, −48.0188888889 W, 27 May 2011, P. P. U. Aquino. DZSJRP 23119 (3, 44.70–65.68 mm SL), 5 March 2015, P. P. U. Aquino and J. C. Bagley, same as holotype location. MNRJ 52558 (2, 35.70–56.70 mm SL), 5 March 2015, P. P. U. Aquino and J. C. Bagley, same as holotype location. MZUSP 125832 (1, 62.20 mm SL), 5 March 2015, P. P. U. Aquino and J. C. Bagley, same as holotype location.

5.3 | Diagnosis

H. crulsi is distinguished from the species of *H. cochliodon* super-group by the slender villiform bicuspid teeth (*vs*. robust spoon-shaped teeth) and by the dentary and premaxillary branch angles greater than 90° (*vs*. angles up to 90°); it is distinguished from the remaining congeners of *H. auroguttatus* super-group by the small size of the dentary and premaxillary and low number of teeth (20–46, mean 36) [*vs*. large size of the dentary and premaxillary, with a large number of teeth (20–140, mean 60)] and by the dark blotches over the body and fins (*vs*. pale blotches). The new species is distinguished from the *H. plecostomus* super-group by the abdominal area completely naked (*vs*. abdominal area completely plated) and by the absence of rows of odontodes on keels (*vs*. moderate to well-developed rows of odontodes on keels). *H. crulsi* differs from *H. nigrolineatus*, *H. subcarinatus* and *H. delimai* by the absence of well-developed rows of odontodes on keels (*vs*. moderate to well-developed row of odontodes on keels); from *H. alatus* and *H. tietensis* by dark spots on a light background (*vs*. light spots on a dark background); from *H. denticulatus* and *H. kuarup* by the small number of teeth in the premaxillary and dentary (20–46) (*vs*. 60–205); and from *H. garmani*, *H. latirostris*, *H. lima* and *H. macrops* by the abdominal area completely naked (*vs*. covered with platelets grouped mainly in the median portion). In addition, *H. crulsi* is distinguished from all its congeners by the abdomen mostly naked, dark dots on the body and fins and abdominal area with no spots, except for *Hypostomus nigromaculatus*; from *H. nigromaculatus* by a combination of characters such as abdominal area completely naked (*vs*. naked abdominal area mostly in the central region, with platelets usually concentrated in the cleithral region), and the absence of the claviform shape and well-developed odontodes in the distal portion of the first pectoral-fin ray (*vs*. claviform shaped well-developed odontodes in the distal portion of the first pectoral-fin ray). Finally, *H. crulsi* can be distinguished from *H. cafuringa* by the naked abdominal area (*vs*. abdominal area partially covered with triangle-shaped platelets).

5.4 | Description

Morphometric and meristic data are provided in Table 3. Largest SL 74.57 mm. Highest body depth at origin of dorsal fin. Largest body width at cleithral region, tapering progressively towards caudal peduncle; cleithral width greater than head depth.

Dorsal profile of body straight from snout tip to nostril insertion; convex from nostrils to origin of dorsal fin; straight along base of the dorsal fin; slightly concave from base of last ray of the dorsal-fin to caudal-fin base. Ventral profile of body almost straight from snout tip to origin of pelvic-fin; postero-dorsally inclined from the origin of the pelvic fin to origin of the anal fin. Caudal peduncle laterally

FIGURE 6 *Hypostomus crulsi*, CIUNB 1497, holotype, 62.3 mm SL; Brazil: Distrito Federal: Brasília: Taquara stream, upper Paraná river basin

compressed, trapezoid-shaped anterior region and ellipsoid-shaped posterior region, both in cross-section.

Slightly depressed head, moderately broad and with rounded snout in dorsal view. Mesethmoid forming a light, rounded crest from tip of snout to region between nostrils. Head with lateral crest from nostrils to posterior margin of compound pterotic; distinctively raised to front of posterorbital region and poorly developed along compound pterotic. Posterior process of parieto-supraoccipital plate delimited by double or triple predorsal plate in some specimens. Axis-shaped operculum with small and undeveloped odontodes. Slightly noticeable facial plates with moderately sized odontodes. Eyes dorsolaterally positioned, with diameter of 14.8%–25% of head length. Moderately sized round oral disc. Outer edge of upper lip without plates, but with small odontodes forming lateral lines in anterior region of lip. Maxillary barbel slightly larger than or equal to eye diameter, attached to lip in proximal region, without ornamentation. Premaxillary teeth 35–48; dentary teeth 37–45. Dentary branches of medium length, forming an angle of *c*. 140–155° to each other. Bicuspid thin teeth curved inward distally; lanceolate, medial cusp considerably larger than pointed lateral cusp. Teeth crown bent ventrally.

Snout tip dorsally covered by small plates and odontodes, completely naked in anteroventral portion, except for two lateral spots of very small plates with odontodes. Ventral surface of head naked. Five lateral plate series: dorsal series with 7–8 plates (mode 8), limiting the naked area along the base of the dorsal fin; mid-dorsal series with 23–24 plates (mode 23); median series with perforated plates 24–26 (mode 25); mid-ventral series with 24–26 plates (mode 24); ventral series with 19–21 plates (mode 20), starting at insertion of pelvic fin or slightly posterior; two ventral plates along base of anal fin, and 11–12 (mode 11) ventral plates from that point of caudal fin. Dorsal, mid-dorsal, mid-ventral plate series without longitudinal keels. Abdomen completely naked, except for few, small plates restricted to lateral region of body between origin of pectoral and pelvic fin. Preanal plaque missing.

Dorsal fin II, 7; moderate to small size; flexible thorn, its distal border almost straight to slightly convex; distal tip not reaching adipose fin when adpressed. Well-developed adipose-fin spine, usually straight, with distal tip depressed and not reaching upper caudal-fin ray. Pectoral fin I, 6; distal border straight. Pectoral spine robust, slightly curved, with rounded tip and generally with inwardly curved odontodes, slightly hypertrophied; odontodes positioned in larger distal region in larger individuals. Pectoral spine reaching beyond pelvic-fin insertion. Pelvic fin i, 5; and with slightly rounded distal border. Unbranched pelvic-fin ray curved inward, surpassing origin of unbranched ray of anal fin when adpressed. Anal fin i, 4; distal tip of posterior rays reaching fifth plate posterior to origin of adpressed anal fin. Caudal fin i, 7 + 7, i; with moderately strong unbranched rays and lower lobe larger than upper lobe.

FIGURE 7 Live specimen of *Hypostomus crulsi*, Brazil: Distrito Federal: Taquara stream, upper Paraná river basin

5.5 | Colour in alcohol

Colour of dorsal and lateral surfaces usually dark brown, varying to light brown, homogeneous on head and trunk; light-brown spotless ventral surface, lighter along head (Figure 6). Dorsal and lateral surface of head and body with round spots. Spots on head smaller than or equal to diameter of eye, slightly enlarged on trunk and caudal peduncle. Spots vary in concentration mainly in head region, with juveniles having spots that are more distant from each other. Some specimens have five dark oblique bars in the lateral region, stress colouration, with the first bar in the posterior region of the head, originating at the insertion of the dorsal-fin unbranched ray, the second bar in the last three branched rays of the dorsal fin, third bar in the insertion of the radius of the adipose fin, fourth in the posterior region of the caudal peduncle and fifth in the posterior region of the rays of the caudal fin.

5.6 | Colour in life

Description based on field observations of various specimens and images of live specimens (Figure 7). General body colour light brown or yellowish with slightly orange. Conspicuous, round, black spots on body, fins and radial membranes similar to colour in specimens preserved in alcohol. Ventral surface of head and abdomen light brown, without dark spots.

5.7 | Distribution

H. crulsi is known only from the headwater streams of the São Bartolomeu River, a tributary of the Corumbá River, drainage of the Paranaíba River, upper Paraná River basin, central Brazil (Figure 5).

5.8 | Natural history

H. crulsi were captured in headwater streams of the São Bartolomeu River, in 4–7 m wide and 0.4–1.0 m deep sections, with rocky bottom and gravel, transparent water, medium-to-fast water stream habitats and relief being quite rugged with altitudes ranging from 898 to

1078 m a.s.l. The riparian vegetation of these streams is mostly dense and is inserted within the Cerrado domain, or central Brazilian dry-diagonal savanna. Part of the sampled areas are located within environmental conservation units, but the other sampling points are in areas of major anthropogenic influence (*e.g.*, with urban sprawl, pollution and crops). *H. crulsi* was predominantly associated with stones, which can make sampling them difficult.

Specimens of *H. crulsi* co-occur with *Characidium gomesi* Travassos, 1956, *Characidium xanthopterum* Silveira, Langeani, da Graça, Pavanelli and Buckup, 2008, *Characidium zebra* Eigenmann, 1909, *Hasemania hanseni* (Fowler, 1949), *Knodus moenkhausii* (Eigenmann & Kennedy, 1903), *Microlepidogaster longicolla* Calegari and Reis, 2010, *Neoplecostomus corumba* Zawadzki, Pavanelli and Langeani, 2008, *Phalloceros harpagos* Lucinda, 2008, *Piabina argentea* Reinhardt, 1867, and the undescribed species of *Astyanax* Baird and Girard, 1854, and *Characidium* Reinhardt, 1867, in the type of location. *H. crulsi* also occurs sympatrically with *Aspidoras fuscoguttatus* Nijssen and Isbrücker, 1976, *Astyanax* gr. *scabripinnis* (Jenyns, 1842), *Piabarchus stramineus* (Eigenmann, 1908), *Crenicichla britskii* Kullander, 1982, *Hyphessobrycon eques* (Steindachner, 1882), *Hypostomus* cf. *ancistroides* (Ihering, 1911), *Kolpotocheirodon theloura* Malabarba and Weitzman, 2000, *Lepomis gibbosus* (Linnaeus, 1758), *M.* cf. *aurantia* Bertaco, Jerep and Carvalho, 2011, *Planaltina myersi* Böhlke, 1954, *P. reticulata* Peters, 1859, and *Rhamdia quelen* (Quoy and Gaimard, 1824) at other sampling localities.

5.9 | Etymology

The specific epithet *crulsi*, an adjective, honours Luiz Ferdinando Cruls (1848–1908), a Belgian engineer and naturalized Brazilian who served as the director of the Imperial Observatory of Rio de Janeiro. He led the Central Plateau Exploration Commission of Brazil, which was responsible for demarcating an area for the installation of the future capital of Brazil. In the chosen region, the city of Brasília was built in 1960 and currently comprises the known distribution of *H. crulsi*.

6 | DISCUSSION

GRRF analyses of the present study supported the phylogenetic hypotheses and candidate species interpretations of Bagley *et al.* (2021) by identifying several diagnostic characters for *H. cafuringa* and *H. crulsi*. The results clearly show that *H. cafuringa* is distinguished from all of its congeners by a set of diagnostic characters, namely its deeper caudal peduncle depth (−0.33–0.25) [*vs.* shorter caudal peduncle depth (−0.43–0.21)], shorter first pectoral-fin ray length (0.07–0.13) [*vs.* longer first pectoral-fin ray length (0.03–0.23)] and shorter dorsal-fin base length (−0.02–0.07) [*vs.* longer dorsal-fin base length (−0.08–0.21)] (see Figure 1c; Table 1). On the contrary, it is shown that *H. crulsi* can be distinguished from all of its congeners by a set of characters, including, mainly, a shorter first pelvic-fin ray length (−0.04–0.11) [*vs.* longer first pelvic-fin ray length (0.01–0.18)], shorter first pectoral-fin ray length (−0.01–0.13) [*vs.* longer first pectoral-fin ray length (0.03–0.23)] and smaller body size (2.79–6.22) [*vs.* larger body size (3.19–9.02)]. In addition, considering the two species described here, the analyses showed that *H. cafuringa* differs from *H. crulsi* by a set of characteristics, including a greater caudal peduncle depth (−0.33–0.25) [*vs.* smaller caudal peduncle depth (−0.37–0.26)] and a larger series of median plates (25–27) [*vs.* smaller series of median plates (24–26)]. All values presented from body size represent isometric size, whereas the remaining morphometric variables are size adjusted (see the "Materials and methods" section for further details).

The practice of accurately and rigorously describing new species through alpha-taxonomy is critical for improving biodiversity accounting in the context of the current biodiversity crisis and also provides a basis for using organisms as model systems in various disciplines of the biological sciences (Drew, 2011; Wheeler, 2004; Wilson, 1985). The authors of this study set out to test the hypothesis that populations of *Hypostomus* from central Brazil that were identified as phylogenetically distinct, and therefore in need of taxonomic reassessment, in recent molecular studies (Bagley *et al.*, 2019; Bagley *et al.*, 2021) represent new species. Apparently, *H. cafuringa* was found only in the headwaters of the Maranhão River, in the Federal District region. *H. crulsi* has been registered only in the headwaters of the Paranoá River, a sub-basin of the upper Paraná River, and curiously, this sub-basin is one of the most septentrional headwaters of the upper Paraná River.

H. cafuringa and *H. crulsi* are small suckermouth-armoured catfish species distributed in the headwater streams of the Distrito Federal that drain into the upper Tocantins and upper Paraná rivers, respectively. Several other small body-sized species have previously been described in the genus *Hypostomus*, *e.g.*, *H. nigromaculatus*, *H. careopinnatus*, *H. velhochico* and *H. yaku* (Martins *et al.*, 2012; Martins *et al.*, 2014; Schubart, 1964; Zawadzki *et al.*, 2017a). This is consistent with literature showing that fast-flowing lotic environments are often associated with smaller species (Lavin & McPhail, 1993; Schlosser, 1987). The rivers and streams of central Brazil are characterized by nutrient-poor, acidic waters with high oxygen concentrations and low electrical conductivity (Padovesi-Fonseca, 2005). *Hypostomus* species that occur in fast-flowing and rocky-bottom environments are generally characterized by the total or partial absence of ventral plates, as observed in *H. kuarup*, *H. yaku*, *H. leucophaeus* and the two new species described here.

Populations of *H. cafuringa* and *H. crulsi* appear to exhibit similar geographical-range sizes and levels of local abundance and therefore are considered to be under similar levels of conservation threat. Both of these species mainly occur in Brazilian protected areas (EPAs), in addition to other small headwater streams in central Brazil. *H. cafuringa* occurs in the Gama-Cabeça-de-Veado EPA established in 1986 (decree no. 9.417/1986), whereas *H. crulsi* occurs in the Cafuringa EPA established in 1988 (decree no. 11.123/1988). Although these EPAs allow sustainable use and conservation of biodiversity and natural resources, these conserved areas are also fragmented by urban and agricultural development. The regions of occurrence of the new species suffer particularly great anthropogenic pressure along the edges of these EPAs, which could negatively influence their

populations now or in the future by reducing habitat area, water quality or migration and gene flow between populations that is needed to maintain species cohesion (Blanchet *et al*., 2010; Fahrig, 2003).

Compared with the species of *Hypostomus* from the Amazon basin that are characterized by a light background colour with dark spots, *H. cafuringa* is distinguished mainly by the absence of keels with odontodes along the lateral series of plates, by the abdominal area partially naked and by a deep caudal peduncle. This new species also differs morphologically from other species with pale spots of the Tocantins River basin, *H. delimai*, *H. faveolus* and *Hypostomus krishnamurtii*. Compared with *Hypostomus* species with dark spots that occur in the La Plata system, *H. crulsi* is distinguished mainly by the absence of hypertrophied odontodes forming keels along the lateral series of plates, abdominal area partially naked and a shorter first pectoral-fin ray length. Despite shared characteristics, *H. cafuringa* and *H. crulsi* are easily distinguished from all other species of *Hypostomus*. In addition, *H. cafuringa* and *H. crulsi* fit into the *H. regani* group of the La Plata system, a clade within the *H. auroguttatus* supergroup *sensu* Jardim de Queiroz *et al*. (2020).

ACKNOWLEDGEMENTS

We are grateful to Antonio Aguiar, Reginaldo Constantino and Roberto Reis for useful contributions to the manuscript. We thank Antonio Cardoso, Carol Azevedo, Gabriel Caputo, Glauber Cunha, Henrique Monteiro, Laís Machado, Lucas Damásio and Thiago B. d'Araujo Couto for assistance with fieldwork. We also thank Antonio Cardoso for drawing the suckermouth catfish illustration used in Figures 1, 2, and S1. We thank Alexandre Ribeiro (CPUFMT), Claudio Oliveira (LBP), Bruno Melo (LBP), Margarete S. Lucena (MCP), Paulo Buckup (MNRJ), Marcelo Britto (MNRJ), Fernando Jerep (MZUEL), Oscar Shibatta (MZUEL), Alessio Datovo (MZUSP), Michel Donato (MZUSP), Osvaldo Oyakawa (MZUSP), Arthur de Lima (MZUSP), Carla Pavanelli (NUP), Cláudio Zawadzki (NUP), Marli Campos (NUP), Juliana Wingert (UFRGS), Luiz Malabarba (UFRGS), Paulo Lucinda (UNT) and Francisco Severo (ZUFMS) for loaning comparative material and hosting our museum visits. G.R.C. thanks Coordenação de Aperfeiçoamento de Pessoal de Nível Superior (CAPES), Conselho Nacional de Desenvolvimento Científico e Tecnológico (CNPq), Fundação de Apoio à Pesquisa do Distrito Federal (FAPDF) and the USAID's PEER programme under cooperative agreement AID-OAA-A-11-00012 for financial support. F.L. thanks Conselho Nacional de Desenvolvimento Científico e Tecnológico (CNPq proc. 305756/2018-4) for financial support. Y.F.F.S. thanks Fundação de Apoio à Pesquisa do Distrito Federal (FAPDF proc. 00193.0000 0926/2018-86) and Coordenação de Aperfeiçoamento de Pessoal de Nível Superior (CAPES) for a scholarship.

AUTHOR CONTRIBUTIONS

Y.F.F.S., G.R.C. and P.P.U.A. conceived and designed the study. Y.F.F.S., J.C.B. and P.P.U.A. conducted fieldwork and organized museum collections. Y.F.F.S. generated the data. Y.F.F.S. and G.R.C. analysed the data. Y.F.F.S. wrote the draft of the manuscript, and G.R.C., F.L., J.C.B. and P.P.U.A. provided edits and comments on the manuscript. Y.F.F.S., F.L. and G.R.C. obtained funding for the study. All authors read and approved the final manuscript.

ORCID

Yan F. F. Soares https://orcid.org/0000-0002-7151-141X
Pedro De Podestà Uchôa de Aquino https://orcid.org/0000-0002-9185-2019
Justin C. Bagley https://orcid.org/0000-0001-6737-8380
Francisco Langeani https://orcid.org/0000-0001-7376-4798
Guarino R. Colli https://orcid.org/0000-0002-2628-5652

REFERENCES

Alkmim, F. F. (2015). Geological background: A tectonic panorama of Brazil. In B. C. Vieira, A. A. R. Salgado, & L. J. C. Santos (Eds.), *Landscape and landforms of Brazil*. Dordrecht, Netherlands: Springer.

Aquino, P. P. U., & Colli, G. R. (2017). Headwater captures and the phylogenetic structure of freshwater fish assemblages: A case study in Central Brazil. *Journal of Biogeography*, *44*, 207–216.

Aquino, P. P. U., & Couto, T. B. A. (2010). Pisces, Teleostei, Characiformes, Characidae, *Hasemania crenuchoides* Zarske and Géry, 1999, *Hyphessobrycon balbus* Myers, 1927 and *Oligosarcus planaltinae* Menezes and Géry, 1983: New records in Distrito Federal, Central Brazil. *Check List*, *6*, 594.

Aquino, P. P. U., Schneider, M., Silva, M. J. M., Fonseca, C. P., Arakawa, H. B., & Cavalcanti, D. R. (2009). Ictiofauna dos córregos do Parque Nacional de Brasília, bacia do alto rio Paraná, Distrito Federal, Brasil Central. *Biota Neotropica*, *9*, 217–230.

Armbruster, J. W. (2004). Phylogenetic relationships of the suckermouth armoured catfishes (Loricariidae) with emphasis on the Hypostominae and the Ancistrinae. *Zoological Journal of the Linnean Society*, *141*, 1–80.

Bagley, J. C., Aquino, P. P. U., Breitman, M. F., Langeani, F., & Colli, G. R. (2019). DNA barcode and minibarcode identification of freshwater fishes from Cerrado headwater streams in Central Brazil. *Journal of Fish Biology*, *95*, 1046–1060.

Bagley, J. C., de Aquino, P. P. U., Hrbek, T., Hernandez-Rangel, S., Langeani, F., & Colli, G. R. (2021). Using ddRAD-seq phylogeography to test for genetic effects of headwater river capture in suckermouth armored catfish (Loricariidae: *Hypostomus*) from the central Brazilian shield. *bioRxiv*, *2021.04.18.440224*, 1–58. https://doi.org/10.1101/2021.04.18.440224.

Barros, J. G. C. (1993). Caracterização geomorfológica e hidrogeológica do Distrito Federal. In M. P. Pinto (Ed.), *Cerrado: Caracterização, ocupação e perspectivas* (pp. 265–283). Brasília, Distrito Federal, Brazil: Editora Universidade de Brasília.

Bickford, D., Lohman, D. J., Sodhi, N. S., Ng, P. K. L., Meier, R., Winker, K., … Das, I. (2007). Cryptic species as a window on diversity and conservation. *Trends in Ecology & Evolution*, *22*, 148–155.

Bitencourt, J. D., Affonso, P., Giuliano-Caetano, L., & Dias, A. L. (2011). Identification of distinct evolutionary units in allopatric populations of *Hypostomus cf. wuchereri* Gunther, 1864 (Siluriformes: Loricariidae): Karyotypic evidence. *Neotropical Ichthyology*, *9*, 317–324.

Blanchet, S., Rey, O., Etienne, R., Lek, S., & Loot, G. (2010). Species-specific responses to landscape fragmentation: Implications for management strategies. *Evolutionary Applications*, *3*, 291–304.

Boeseman, M. (1968). The genus *Hypostomus* Lacépède 1803 and its Surinam representatives (Siluriformes, Loricariidae). *Zoologische Verhandelingen*, *99*, 1–89.

Breiman, L. (2001). Random forests. *Machine Learning*, *45*, 5–32.

Breitman, M. F., Domingos, F. M. C. B., Bagley, J. C., Wiederhecker, H. C., Ferrari, T. B., Cavalcante, V. H. G. L., … Colli, G. R. (2018). A new

species of *Enyalius* (Squamata, Leiosauridae) endemic to the Brazilian Cerrado. *Herpetologica*, *74*, 355–369.

Bruton, M. N. (1996). Alternative life-history strategies of catfishes. *Aquatic Living Resources*, *9*, 35–41.

Burnaby, T. P. (1966). Growth-invariant discriminant functions and generalized distances. *Biometrics*, *22*, 96–110.

Cardoso, Y. P., Brancolini, F., Paracampo, A., Lizarralde, M., Covain, R., & Montoya-Burgos, J. I. (2016). *Hypostomus formosae*, a new catfish species from the Paraguay river basin with redescription of *H. boulengeri* (Siluriformes: Loricariidae). *Ichthyological Exploration of Freshwaters*, *27*, 9–23.

Cardoso, Y. P., Brancolini, F., Protogino, L., Paracampo, A., Bogan, S., Posadas, P., & Montoya-Burgos, J. I. (2019). An integrated approach clarifies the cryptic diversity in *Hypostomus* Lacépède 1803 from the lower La Plata Basin. *Anais da Academia Brasileira de Ciências*, *91*, e20180131.

Cardoso, Y. P., Jardim de Queiroz, L., Bahechar, I. A., Posadas, P. E., & Montoya-Burgos, J. I. (2021). Multilocus phylogeny and historical biogeography of *Hypostomus* shed light on the processes of fish diversification in La Plata Basin. *Scientific Reports*, *11*(5073), 1–14. https://doi.org/10.1038/s41598-021-83464-x.

Castro, R. M. C. (1999). Evolução da ictiofauna de riachos sul-americanos: Padrões gerais e possíveis processos causais. In E. P. Caramaschi, R. Mazzoni, & P. R. Peres-Neto (Eds.), *Ecologia de peixes de riacho* (pp. 139–155). Rio de Janeiro, Brasil: PPGE-UFRJ.

Delic, T., Trontelj, P., Rendos, M., & Fiser, C. (2017). The importance of naming cryptic species and the conservation of endemic subterranean amphipods. *Scientific Reports*, *7*, 1–12.

Deng, H. (2013). Guided random forest in the RRF package. *arXiv*, *1306.0237*, 1–2 https://arxiv.org/abs/1306.0237.

Deng, H. T., & Runger, G. (2013). Gene selection with guided regularized random forest. *Pattern Recognition*, *46*, 3483–3489.

Drew, L. W. (2011). Are we losing the science of taxonomy? *Bioscience*, *61*, 942–946.

Endo, K. S., Martinez, E. R. M., Zawadzki, C. H., Paiva, L. R. S., & Júlio Júnior, H. F. (2012). Karyotype description of possible new species of the *Hypostomus ancistroides* complex (Teleostei: Loricariidae) and other Hypostominae. *Acta Scientiarum. Biological Sciences*, *34*, 181–189.

Fahrig, L. (2003). Effects of habitat fragmentation on biodiversity. *Annual Review of Ecology, Evolution, and Systematics*, *34*, 487–515.

Ferraris, C. J. (2007). Checklist of catfishes, recent and fossil (Osteichthyes: Siluriformes), and catalogue of siluriform primary types. *Zootaxa*, *1418*(1), 1–548. https://doi.org/10.11646/zootaxa.1418.1.1.

Fricke, R., Eschmeyer, W. N. & Fong, J. D. (2019). Species by Family/Subfamily. Available at: http://researcharchive.calacademy.org/research/ichthyology/catalog/SpeciesByFamily.asp.

Froese, R., & Pauly, D. (2019). *FishBase*. Stockholm, Sweden: World Wide Web Electronic Publication Available at: www.fishbase.org.

Griffiths, S. P. (2000). The use of clove oil as an anaesthetic and method for sampling intertidal rockpool fishes. *Journal of Fish Biology*, *57*, 1453–1464.

Jardim de Queiroz, L., Cardoso, Y., Jacot-des-Combes, C., Bahechar, I. A., Lucena, C. A., Py-Daniel, L. R., … Montoya-Burgos, J. I. (2020). Evolutionary units delimitation and continental multilocus phylogeny of the hyperdiverse catfish genus *Hypostomus*. *Molecular Phylogenetics and Evolution*, *145*, 1–15.

Jolicouer, P. (1963). Multivariate generalization of allometry equation. *Biometrics*, *19*, 497–499.

Lavin, P. A., & McPhail, J. D. (1993). Parapatric lake and stream sticklebacks on northern Vancouver Island - disjunct distribution or parallel evolution. *Canadian Journal of Zoology-Revue Canadienne De Zoologie*, *71*, 11–17.

Liaw, A., & Wiener, M. (2002). Classification and regression by randomForest. *R News*, *2*, 18–22.

Lucinda, P. H. F. (2008). Systematics and biogeography of the genus *Phalloceros* Eigenmann, 1907 (Cyprinodontiformes: Poeciliidae: Poeciliinae), with the description of twenty-one new species. *Neotropical Ichthyology*, *6*, 113–158.

Mariguela, T. C., Alexandrou, M. A., Foresti, F., & Oliveira, C. (2013). Historical biogeography and cryptic diversity in the Callichthyinae (Siluriformes, Callichthyidae). *Journal of Zoological Systematics and Evolutionary Research*, *51*, 308–315.

Martins, F. O., Langeani, F., & Zawadzki, C. H. (2014). A new spiny species of *Hypostomus* Lacépède (Loricariidae: Hypostominae) from thermal waters, upper rio Parana basin, Central Brazil. *Neotropical Ichthyology*, *12*, 729–736.

Martins, F. O., Marinho, M. M. F., Langeani, F., & Serra, J. P. (2012). A new species of *Hypostomus* (Siluriformes: Loricariidae) from the upper rio Paraguay basin, Brazil. *Copeia*, *8*, 494–500.

Montoya-Burgos, J. I. (2003). Historical biogeography of the catfish genus *Hypostomus* (Siluriformes: Loricariidae), with implications on the diversification of Neotropical ichthyofauna. *Molecular Ecology*, *12*, 1855–1867.

Murphy, J. C., Jowers, M. J., Lehtinen, R. M., Charles, S. P., Colli, G. R., Peres, A. K., … Pyron, R. A. (2016). Cryptic, sympatric diversity in tegu lizards of the *Tupinambis teguixin* group (Squamata, Sauria, Teiidae) and the description of three new species. *PLoS One*, *11*, e0158542.

Nogueira, C., Buckup, P. A., Menezes, N. A., Oyakawa, O. T., Kasecker, T. P., Neto, M. B. R., & da Silva, J. M. C. (2010). Restricted-range fishes and the conservation of brazilian freshwaters. *PLoS One*, *5*, e11390.

Oyakawa, O. T., Akama, A., & Zanata, A. M. (2005). Review of the genus *Hypostomus* Lacépède, 1803 from rio Ribeira de Iguape basin, with description of a new species (Pisces, Siluriformes, Loricariidae). *Zootaxa*, *921*, 1–27. https://doi.org/10.11646/zootaxa.921.1.1.

Padovesi-Fonseca, C. (2005). Caracterização dos ecossistemas aquáticos do Cerrado. In A. Scariot, J. C. Souza-Silva, & J. M. Felfili (Eds.), *Cerrado: Ecologia, Biodiversidade e Conservação* (pp. 415–429). Brasília, Distrito Federal, Brazil: Ministério do Meio Ambiente.

R Core Team. (2018). *R: A language and environment for statistical computing*. Vienna, Austria: R Foundation for Statistical Computing Available at: https://cran.r-project.org.

Rohlf, F. J., & Bookstein, F. L. (1987). A comment on shearing as a method for "size correction". *Systematic Zoology*, *36*, 356–367.

Roxo, F. F., Ochoa, L. E., Sabaj, M. H., Lujan, N. K., Covain, R., Silva, G. S. C., … Oliveira, C. (2019). Phylogenomic reappraisal of the Neotropical catfish family Loricariidae (Teleostei: Siluriformes) using ultraconserved elements. *Molecular Phylogenetics and Evolution*, *135*, 148–165.

Schaefer, S. A. (1997). The neotropical cascudinhos: Systematics and biogeography of the *Otocinclus* catfishes (Siluriformes: Loricariidae). *Proceedings of the Academy of Natural Sciences of Philadelphia*, *148*, 1–120.

Schlosser, I. J. (1987). The role of predation in age-related and size-related habitat use by stream fishes. *Ecology*, *68*, 651–659.

Schubart, O. (1964). Sobre algumas Loricariidae da bacia do rio Mogi Guaçu (Pisces, Nematognatha). *Boletim do Museu Nacional*, *251*, 1–19.

Silva, G. S. C., Roxo, F. F., Lujan, N. K., Tagliacollo, V. A., Zawadzki, C. H., & Oliveira, C. (2016). Transcontinental dispersal, ecological opportunity and origins of an adaptive radiation in the Neotropical catfish genus *Hypostomus* (Siluriformes: Loricariidae). *Molecular Ecology*, *25*, 1511–1529.

Somers, K. M. (1986). Multivariate allometry and removal of size with principal components-analysis. *Systematic Zoology*, *35*, 359–368.

Souza, C. R., Affonso, P., Bitencourt, J. D., Sampaio, I., & Carneiro, P. L. S. (2018). Species validation and cryptic diversity in the *Geophagus brasiliensis* Quoy & Gaimard, 1824 complex (Teleostei, Cichlidae) from Brazilian coastal basins as revealed by DNA analyses. *Hydrobiologia*, *809*, 309–321.

Stekhoven, D. J., & Buhlmann, P. (2012). MissForest-non-parametric missing value imputation for mixed-type data. *Bioinformatics*, *28*, 112–118.

Todorov, V. (2016). rrcovNA: Scalable robust estimators with high breakdown point for incomplete data. *R package*. Available at: https://CRAN.R-project.org/package=rrcovNA.

Uieda, V. S. C., & Castro, R. M. (1999). Coleta e fixação de peixes de riachos. In E. P. Caramaschi, R. Mazzoni, & P. R. Peres-Neto (Eds.), *Ecologia de Peixes de Riacho* (pp. 1–22). Rio de Janeiro, Brazil: PPGE-UFRJ.

Weber, C. (1985). *Hypostomus dlouhyi*, nouvelle espèce de poisson-chat cuirassé du Paraguay (Pisces, Siluriformes, Loricariidae). *Revue Suisse de Zoologie*, *92*, 955–968.

Wheeler, Q. D. (2004). Taxonomic triage and the poverty of phylogeny. *Philosophical Transactions of the Royal Society of London Series B-Biological Sciences*, *359*, 571–583.

Wilson, E. O. (1985). The biological diversity crisis. *Bioscience*, *35*, 700–706.

Zawadzki, C. H., Birindelli, J. L. O., & Lima, F. C. T. (2008a). A new pale-spotted species of *Hypostomus* Lacépède (Siluriformes: Loricariidae) from the rio Tocantins and rio Xingu basins in Central Brazil. *Neotropical Ichthyology*, *6*, 395–402.

Zawadzki, C. H., de Oliveira, R. R., & Debona, T. (2013). A new species of *Hypostomus* Lacépède, 1803 (Siluriformes: Loricariidae) from the rio Tocantins-Araguaia basin, Brazil. *Neotropical Ichthyology*, *11*, 73–80.

Zawadzki, C. H., Oyakawa, O. T., & Britski, H. A. (2017a). *Hypostomus velhochico*, a new keeled *Hypostomus* Lacépède, 1803 (Siluriformes: Loricariidae) from the rio São Francisco basin in Brazil. *Zootaxa*, *4344*, 560–572.

Zawadzki, C. H., Ramos, T. P. A., & Sabaj, M. (2017b). *Hypostomus sertanejo* (Siluriformes: Loricariidae), new armoured catfish species from North-Eastern Brazil. *Journal of Fish Biology*, *91*, 317–330.

Zawadzki, C. H., Weber, C., & Pavanelli, C. S. (2008b). Two new species of *Hypostomus* Lacépède (Teleostei: Loricariidae) from the upper rio Paraná basin, Central Brazil. *Neotropical Ichthyology*, *6*, 403–412.

Zawadzki, C. H., Weber, C., & Pavanelli, C. S. (2010). A new dark-saddled species of *Hypostomus* (Siluriformes: Loricariidae) from the upper rio Paraguay basin. *Neotropical Ichthyology*, *8*, 719–725.

SUPPORTING INFORMATION

Additional supporting information may be found online in the Supporting Information section at the end of this article.

How to cite this article: Soares, Y. F. F., de Aquino, P. D. P. U., Bagley, J. C., Langeani, F., & Colli, G. R. (2021). Two new species of *Hypostomus* suckermouth-armoured catfishes (Teleostei: Loricariidae) from central Brazil. *Journal of Fish Biology*, 1–16. https://doi.org/10.1111/jfb.14777